Citation: CPT: Pharmacometrics & Systems Pharmacology (2012) 1, e17; doi:10.1038/psp.2012.18

www.nature.com/psp

ORIGINAL ARTICLE

Nonlinear Population Pharmacokinetics of Sirolimus in Patients With Advanced Cancer

K Wu[1], EEW Cohen[1,3], LK House[1], J Ramírez[1], W Zhang[1], MJ Ratain[1,2,3] and RR Bies[4]

Sirolimus, the prototypical inhibitor of the mammalian target of rapamycin, has substantial antitumor activity. In this study, sirolimus showed nonlinear pharmacokinetic characteristics over a wide dose range (from 1 to 60 mg/week). The objective of this study was to develop a population pharmacokinetic (PopPK) model to describe the nonlinearity of sirolimus. Whole blood concentration data, obtained from four phase I clinical trials, were analyzed using a nonlinear mixed-effects modeling (NONMEM) approach. The influence of potential covariates was evaluated. Model robustness was assessed using nonparametric bootstrap and visual predictive check approaches. The data were well described by a two-compartment model incorporating a saturable Michaelis–Menten kinetic absorption process. A covariate analysis identified hematocrit as influencing the oral clearance of sirolimus. The visual predictive check indicated that the final pharmacokinetic model adequately predicted observed concentrations. The pharmacokinetics of sirolimus, based on whole blood concentrations, appears to be nonlinear due to saturable absorption.

CPT: Pharmacometrics & Systems Pharmacology (2012) **1,** e17; doi:10.1038/psp.2012.18; advance online publication 5 December 2012

Sirolimus (rapamycin) is commonly prescribed as an immunosuppressant and is indicated for the prevention of allograft rejection.[1] As the prototypical inhibitor of the mammalian target of rapamycin, sirolimus (like other mammalian target of rapamycin inhibitors) has substantial antitumor activity both in animals and humans.[2–6] Sirolimus has low bioavailability (14% on average) and a long terminal elimination half-life of ~62 h.[7] Studies in transplant patients have demonstrated marked interindividual pharmacokinetic variability, resulting in the widespread use of therapeutic drug monitoring based on whole blood concentrations.[8–13]

There are several publications regarding the pharmacokinetics of sirolimus in transplant patients, although none have explicitly incorporated the nonlinear pharmacokinetic characteristics into a mixed-effects population model.[8–12] Jiao *et al.*[13] reported the nonlinearity in the pharmacokinetics of sirolimus, but they were unable to develop an explicit model to describe this due to limited measurements. Recently, several phase I trials of sirolimus in patients with cancer were completed, including the intermittent administration of higher doses.[14,15] These studies provided the opportunity to investigate the nonlinearity in sirolimus disposition using whole blood concentration measurements. The detection and characterization of nonlinearities provided by population modeling allows a better understanding of how a drug should be used in clinical practice.[16]

The objective of this study was to develop a population pharmacokinetic (PopPK) model for sirolimus, while exploring possible nonlinear absorption characteristics in whole blood measurements. These measurements were obtained from clinical trials of patients with advanced cancer who received sirolimus in a wide range of dosages (1–60 mg/week). This is the first PopPK report of sirolimus in patients with advanced cancer.

RESULTS

A total of 563 concentration data points from 76 patients with advanced solid tumors enrolled in four different phase I trials at The University of Chicago were available for the analysis.[14,15] An example of the data records is provided in the **Supplementary Table S1** online.

Noncompartmental analysis

Figure 1a,b demonstrates the nonlinearity of sirolimus pharmacokinetics. The slope of dose-normalized area under the curve $(\mathrm{AUC})_{0-\infty}$ vs. dose differed significantly from zero ($P < 0.01$), indicating that the drug exposure did not increase linearly with dose. The terminal elimination half-life did not deviate significantly from zero ($P > 0.05$), suggesting that the elimination is linear over the dose range in this study.

Nonlinear PopPK model

Sirolimus concentration vs. time curves were best described using a two-compartment model with a saturable absorption model (Michaelis–Menten equation) (**Figure 2**). The base model was characterized by the following expressions:

$$\frac{\mathrm{d}A_1}{\mathrm{d}t} = -\frac{Vm \times A_1}{Km + A_1}$$

$$\frac{\mathrm{d}A_2}{\mathrm{d}t} = \frac{Vm \times A_1}{Km + A_1} - \frac{\mathrm{CL}_1}{V_1} \times A_2 - \frac{\mathrm{CL}_2}{V_1} \times A_2 + \frac{\mathrm{CL}_2}{V_2} \times A_3$$

$$\frac{\mathrm{d}A_3}{\mathrm{d}t} = \frac{\mathrm{CL}_2}{V_1} \times A_2 - \frac{\mathrm{CL}_2}{V_2} \times A_3$$

where A_1, A_2, and A_3 are the amounts of drug in the intestinal lumen and central and peripheral compartments. Vm (μg/l·h)

[1]Department of Medicine, The University of Chicago, Chicago, Illinois, USA; [2]Committee on Clinical Pharmacology and Pharmacogenomics, The University of Chicago, Chicago, Illinois, USA; [3]Cancer Research Center, The University of Chicago, Chicago, Illinois, USA; [4]Division of Clinical Pharmacology and Indiana CTSI, Indiana University School of Medicine, Indianapolis, Indiana, USA. Correspondence: MJ Ratain, (mratain@medicine.bsd.uchicago.edu)
Received 2 August 2012; accepted 9 October 2012; advance online publication 5 December 2012. doi:10.1038/psp.2012.18

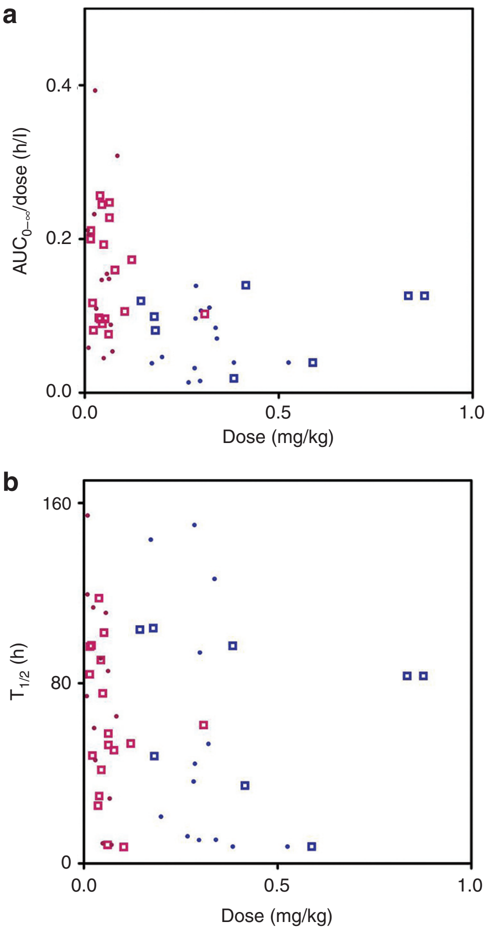

Figure 1 The ratio of area under the curve $(AUC)_{0-\infty}$ and dose $(AUC_{0-\infty}/dose)$ (**a**) and terminal elimination half-life (**b**) vs. doses. Males and females are represented by dots and squares. The data from trials 2 (dose range 1–16 mg) and 3 (dose range 15–35 mg) are shown in pink and blue.

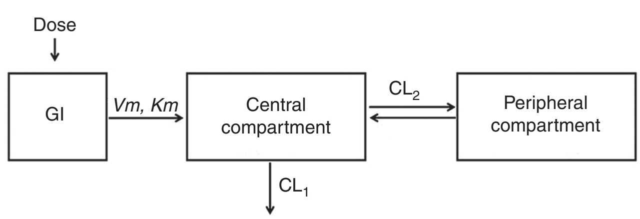

Figure 2 Two-compartment model with a saturable Michaelis–Menten kinetic absorption. CL_1, clearance from central compartment; CL_2, clearance between central and peripheral compartments; GI, gastrointestinal tract; *Km*, the amount at 50% of *Vm*; *Vm*, maximum absorption rate.

is the maximum absorption rate and *Km* (mg) is the drug amount at 50% of *Vm*. *Vm*, *Km*, CL_1, V_1, CL_2, and V_2 were fitted. At 0 h, A_1 = dose, and A_2 and $A_3 = 0$.

A combined proportional and additive error model was used to describe the residual unexplained variability representing the variance between the observed concentrations and those predicted by the model:

$$C_{obs} = C_{pred} \cdot (1 + \varepsilon_1) + \varepsilon_2$$

where C_{obs} and C_{pred} are the observed and predicted concentrations. ε_1 and ε_2 are randomly distributed variables with a mean of zero and variances of σ_1^2 and σ_2^2 accounted for the residual variabilities.

The estimated PopPK parameters are listed in **Table 1**. The relative standard errors of parameter estimates ranged from 8.17% to 55.4%. **Figure 3** shows the relationship between the observed and population model–predicted concentrations and the relationship between the observed and individual model–predicted concentrations. The subjects in these studies were outpatients, and undocumented variability in timing of doses may be a significant factor impacting both bias and precision.[17] The M3 method was tried as there were 16 samples (2.0% of all observations) below the limit of quantification.[18] It was not included in our final model because addition of the M3 method did not improve the model fit. Hematocrit was the only significant covariate affecting the apparent clearance of sirolimus (clearance decreased with increasing hematocrit). Drug formulation (liquid vs. solid) did not have a significant impact on the absorption-related parameters.

Model evaluation

The median parameter values resulting from the bootstrap procedure agreed with the estimates from the final population model. This suggests that the parameters in the final model were reasonably well determined and the model was stable. From 1,000 bootstrap runs, 985 minimized successfully and were included in the bootstrap analysis. The results of the bootstrap analysis are summarized in **Table 1**. **Figure 4** shows the median and the 5th and 95th percent prediction intervals from the visual predictive check simulation with the observed data superimposed. These plots show that most of the observed concentrations on all dose levels fell within the 5th–95th percent prediction interval. Observed concentrations <10% lay outside the prediction intervals. The visual predictive check shows that the final model adequately describes the majority of the data.

DISCUSSION

This is the first PopPK study of sirolimus in patients with cancer. Using whole blood concentrations, the data were adequately explained by a Michaelis–Menten absorptive process, which results in increased apparent oral clearance with dose.

In addition, our model demonstrated that the apparent oral clearance of sirolimus was inversely associated with hematocrit, although this has only a modest effect on clearance (e.g., an increase in hematocrit from 35.1% to 44.7% results in a decrease in apparent clearance from 12.9 to 12.4 l/hr). Sirolimus is distributed mostly into red blood cells and very little into plasma (<5%).[19–21] The sequestration of sirolimus, like tacrolimus, into blood cells is believed to be mainly due to the presence of binding proteins such as FK binding protein.[22] Lipid solubility, degree of ionization, molecular size, and hydrogen-bonding ability have been identified as the main determinants for uptake by the red blood cells. The relationship between clearance and hematocrit may reflect the exchange of sirolimus between plasma and red blood cells. This exchange plays

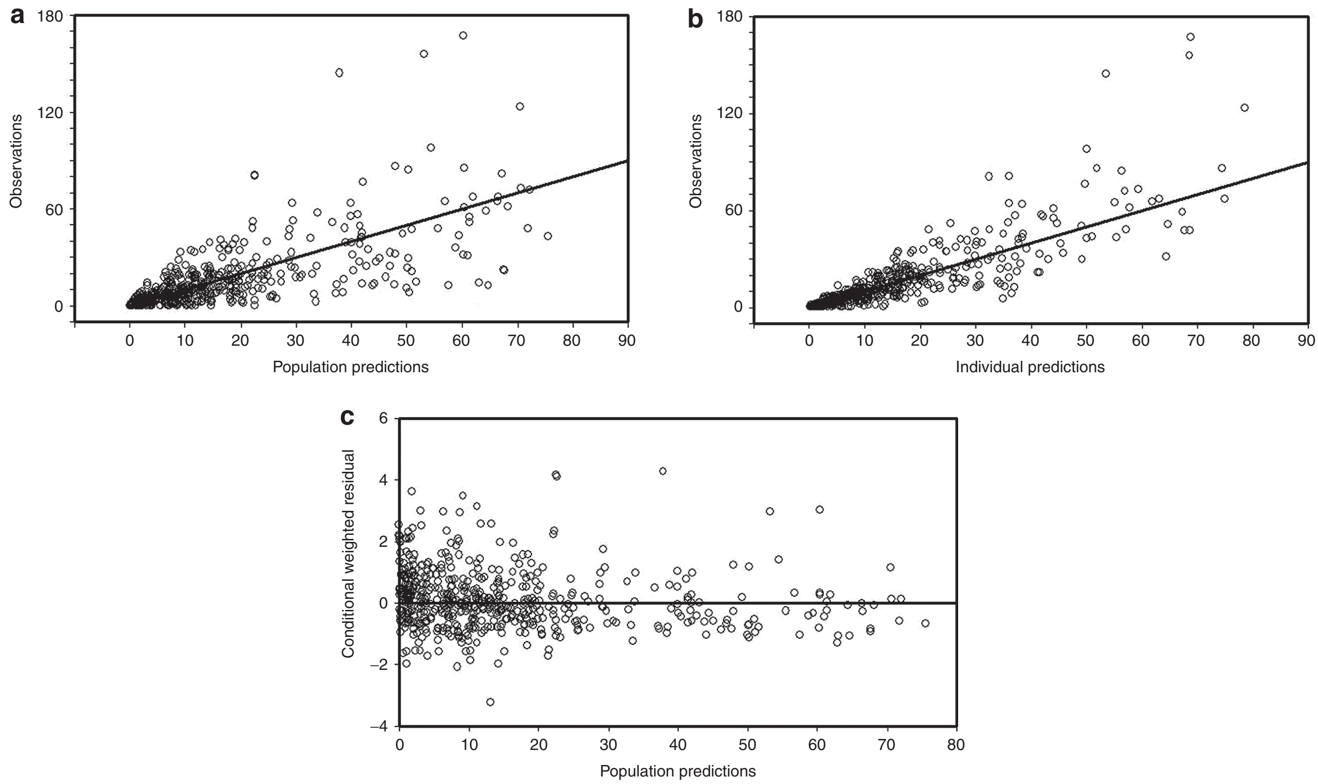

Figure 3 Observed (DV) vs. (**a**) population model predicted and (**b**) individual model predicted concentrations. The solid lines are diagonal lines of identity. (**c**) Conditional weighted residuals vs. population predictions.

Table 1 Final population pharmacokinetic parameter estimates and bootstrap results of sirolimus

		NONMEM	Bootstrap
Parameter (unit)	**Definition**	**Estimate (% SE) (shrinkage)**	**Estimate (% SE)**
$CL_1/F = \theta_1 \times$ (median/hematocrit)$^{\theta_2}$			
θ_1 (l/h)	Typical value of clearance from central compartment	12.9 (16.3%)	12.8 (49.9%)
θ_2	Factor of hematocrit	0.14 (55.4%)	0.11 (22.8%)
V_1/F (l)	Volume of distribution of central compartment	53.4 (38.0%)	59.1 (52.3%)
CL_2/F (l/h)	Clearance between compartments	29.0 (8.17%)	27.8 (10.1%)
V_2/F (l)	Volume of distribution of peripheral compartment	611 (11.3%)	607 (16.4%)
Vm (μg/l·h)	Maximum absorption rate	4.56 (37.7%)	4.61 (41.2%)
Km (mg)	The amount at 50% of *Vm*	13.8 (50.3%)	14.2 (59.3%)
Interindividual variability (%SE) (shrinkage)			
CL_1/F		52.4% (57.8%) (12.5%)	66.7% (70.2%)
V_1/F		52.4 % (57.8%) (24.0%)	66.7% (70.2%)
CL_2/F		70.5% (17.2%) (32.4%)	69.3% (40.9%)
V_2/F		19.3% (177%) (28.0%)	20.5% (150%)
Intraindividual variability (%SE) (shrinkage)			
Proportional (%)		2.17 % (97.0%) (11.1%)	2.53% (15.6%)
Additive (ng/ml)		0.5 (35.5%) (11.9%)	0.48 (30.9%)

The median of hematocrit is 35.1%.
NONMEM, nonlinear mixed-effects modeling.

an important role in its pharmacokinetic behavior.[9] Many other drugs, such as tacrolimus[23] and cyclosporine,[24] also show a correlation between whole blood clearance and hematocrit.[23,24]

In the forward addition process, gender was found to be significantly related with V_1/F (V_1/F for female is 75% of the V_1/F for male), but did not pass the backward elimination. The volume of distribution for the peripheral compartment increased slightly with increasing body weight (the exponent is 0.676); however, the addition of body weight to volume of distribution as a covariate did not result in a statistically significant change in the objective function value (1.589).

Michaelis–Menten kinetics was incorporated in our model to describe the saturable absorption. This is consistent with a previous study on intestinal absorption, which demonstrated a concentration-dependent and saturable transepithelial transport of sirolimus across Caco-2 monolayers.[25] The mechanism of absorption is not very clear, and the model could be further understood once the drug transport mechanisms are elucidated.[25] Cummins *et al.*[26] studied the cellular pharmacokinetics of sirolimus in CYP3A4-transfected Caco-2 cells. They found that the net effect of P-glycoprotein on metabolism was not as great as that expected for sirolimus, a P-glycoprotein substrate, and assumed that there might be multiple transporters involved in sirolimus absorption.

Our model fit the concentration data well. The residual of the pharmacokinetic parameter estimates was acceptable (Table 1). The clearance of central compartment in our

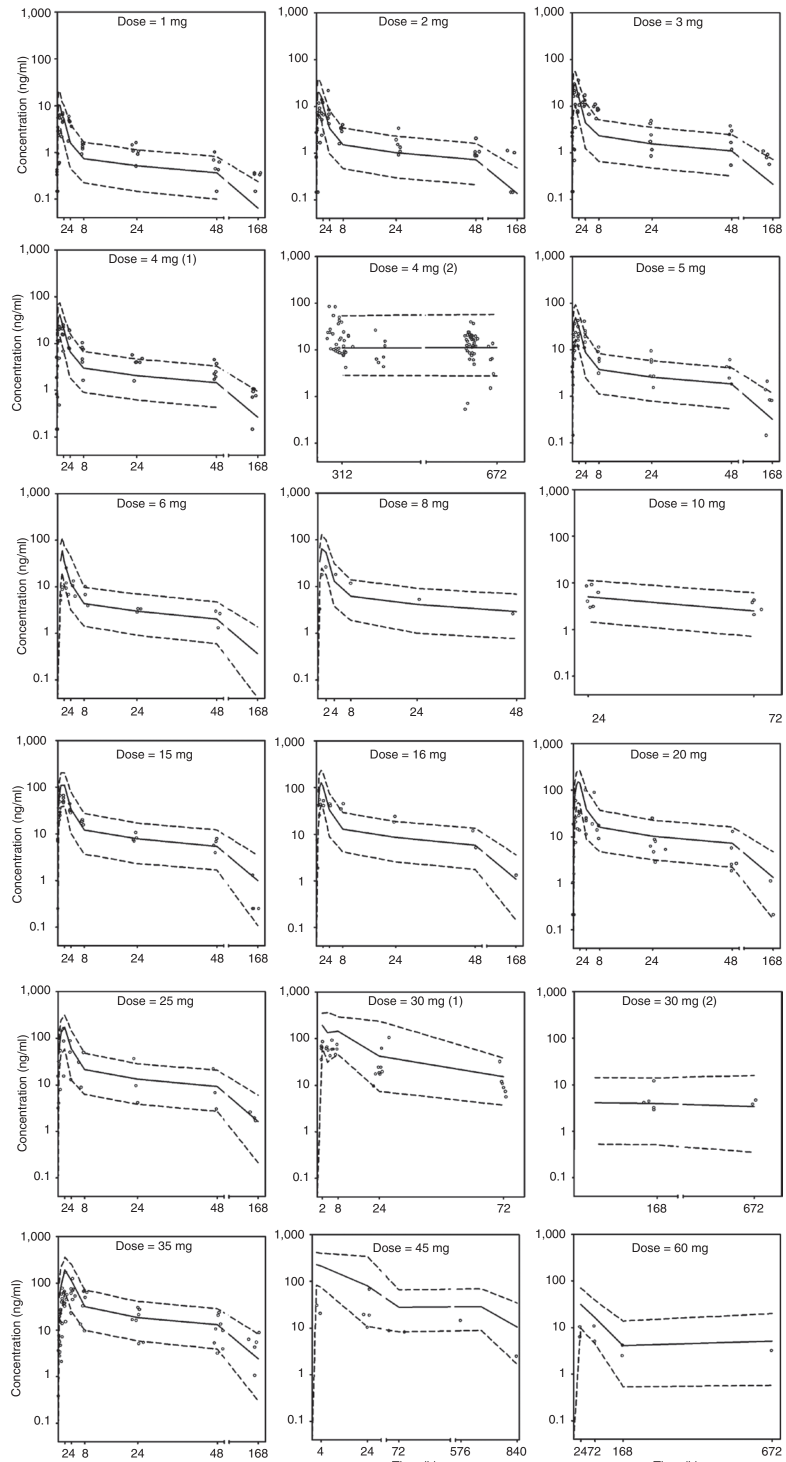

Figure 4 Visual predictive check of the model for all dose levels. The median model predictions are shown by solid lines and 95% prediction intervals are encompassed by the broken lines. The dots present the observed concentrations.

study is comparable with those reported previously (7.9–28.3 l/h).[10,12,20,23] The apparent volume of distribution of the peripheral compartment (tissue) is in the range of values reported in previous studies (11.6–1,350 l).[8–10,12,20,23] Because sirolimus is hydrophobic, it is widely distributed in the lipid membranes of body tissues and the erythrocytes and shows a large apparent volume of distribution.[10,22]

The current PopPK analysis can be used to predict the effect of dose and/or schedule change on the whole blood concentrations of sirolimus. This will facilitate future studies of this agent in addition to providing information that may guide dosing for patients individually.

METHODS

Patients and data collection. The clinical trials were reviewed and approved by The University of Chicago Institutional Review Board.[14,15] Written informed consent was obtained from all patients. The demographic characteristics of the patients are summarized in **Table 2**. Treatment was administered on an outpatient basis according to the treatment schedule listed in **Table 3**. Patients self-administered sirolimus (without food) at the scheduled times per protocol. Patients from trial 1 were given high dose sirolimus. In trials 2 and 3, escalated doses of sirolimus were administered. In trial 4, a fixed sirolimus dose of 4 mg was given. Dosing was independent of body weight. Sirolimus was supplied in liquid form for trials 1, 3, and 4, and in tablet form for trial 2.

Blood sampling and sirolimus analysis. Sirolimus whole blood concentrations were obtained according to the sampling schedule shown in **Table 3**. Samples were stored at −80 °C until analysis by high-performance liquid chromatography combined with tandem mass spectrometry (LC/MS/MS) for trials 2, 3, and 4. The extraction and LC/MS/MS methods are described in **Supplementary Appendix** online. The samples from trial 1 were analyzed using high-performance liquid chromatography and LC/MS/MS. The limit of quantification (in ng/ml) was 2 (trial 1), 0.28 (trials 2 and 3), and 0.49 (trial 4).

Noncompartmental analysis. To evaluate the dose dependence of the pharmacokinetic behavior of sirolimus, $AUC_{0-\infty}$ and half-life were calculated using a noncompartmental pharmacokinetic analysis implemented in the PK Solutions software (version 2.0; Summit Research Services, Montrose, CO). Sirolimus whole blood concentrations from trials 2 and 3 were used for this analysis. To establish dose linearity and proportionality, dose-normalized $AUC_{0-\infty}$ and half-life were analyzed using regression analysis ($\alpha = 0.05$).

Nonlinear PopPK model. An analysis was performed using a nonlinear mixed-effects modeling (NONMEM) approach as implemented in NONMEM (version VII, level 1; ICON, Ellicott City, MD) in conjunction with a gfortran compiler.[27] First-order conditional estimation with interaction and the ADVAN 13 subroutine were applied.

A number of candidate models were assessed in describing the concentration data and apparent nonlinearity of the pharmacokinetics of sirolimus: two-compartment model with Michaelis–Menten elimination; Michaelis–Menten absorption; zero-order absorption and first-order loss in gastrointestinal tract; parallel zero-order and first-order absorption; and Weibull absorption.[8] Mixture distributions were also explored to examine whether the absorption patterns had a multimodal characteristic. Demographic data of the patients, shown in **Table 2**, were tested in the model one by one as candidate covariates on each of the parameters. The final PopPK model was established using the stepwise forward addition and backward elimination method.[28] Comparison of the models was based on the objective function value provided by NONMEM at a significance level of 0.05 (equal to a decrease of 3.84 in the objective function value) for the forward addition and 0.01 (equal to a decrease of 6.63 in the objective function value) for the backward elimination for 1 degree of freedom.

Interindividual variability was described with a statistical model. Pharmacokinetic parameters were expressed by the exponential Eq. 1:

$$P_{ij} = P_{TVj} \cdot \mathrm{Exp}(\eta_{ij})$$

where P_{ij} represents the *j*th basic pharmacokinetic parameter for the *i*th individual, P_{TVj} is the typical population value of the

Table 2 Patient demographics

Characteristic	Mean (range) or *N*
Age (years)	57.7 (22–83)
Body weight (kg)	79.76 (32.8–154.6)
Height (cm)	170.73 (146.0–210.8)
Gender	
Male	39
Female	37
Hematocrit (%)	35.0 (11.8–44.7)
Blood urea nitrogen (mg/dl)	14.9 (5–63)
Total bilirubin (mg/dl)	0.47 (0.1–1.8)
SGOT (U/l)	35.6 (10–138)
SGPT (U/l)	27.5 (3–249)
Alkaline phosphatase (U/l)	178.7 (35–1,119)
Creatinine (mg/dl)	0.85 (0.3–1.4)
GFR (ml/min/BSA)	88.69 (42–>120)
Albumin (g/dl)	3.80 (2.5–4.6)
WBC (K/µl)	7.00 (2.1–27.8)
Red blood cells (M/µl)	3.975 (2.27–7.18)
Hemoglobin (g/dl)	11.83 (7.5–15.7)
Platelets (K/µl)	293.3 (75–896)
Total protein (g/dl)	6.91 (5.3–9.0)
Triglycerides (mg/dl)	113.4 (44–514)
Glucose (mg/dl)	105.9 (51–213)
Cholesterol (mg/dl)	175.7 (94–286)

BSA, body surface area; GFR, glomerular filtration rate; SGOT, serum glutamic oxaloacetic transaminase; SGPT, serum glutamic pyruvic transaminase; WBC, White blood cells.

Table 3 Treatment and sampling schedule for the clinical trials

Trial No.	Treatment	Number of patients	Dose range (mg)	No. of observations	PK sampling time points (days) (h)
1	Once weekly	13	10–60	41	0, 2, 4, 24, 76, 168 (day 1, 2, 4, 8, 25, 29, and 36)[a]
2	Once weekly	36	1–16	619	0, 0.25, 0.5, 1, 2, 4, 8, 24, 48, 168 (day 1)
3	Once weekly	19	15–35	368	0, 0.25, 0.5, 1, 2, 4, 8, 24, 48, 168 (day 1)
4	Once daily	8	4	98	0, 1, 4, 6, 8, 24 (day 14 and 28)

PK, pharmacokinetic.

[a]Sampling schedule is not same among the patients in trial 1.

*j*th parameter, and η_{ij} is realization from a normally distributed interindividual variable with a mean of 0 and an estimated variance of ω_j^2, which is the deviation of P_{ij} from $P_{TV\,j}$. Residual unexplained variability was evaluated using additive, proportional, and their combined error models. The NONMEM code is provided in the **Supplementary Data** online.

Model evaluation. The final model was evaluated using a nonparametric bootstrap and visual predictive check.[29,30] The bootstrap evaluation involved resampling the original data set 1,000 times (sampling with replacement). The median values and the 2.5th and 97.5th percentiles of the parameters obtained by this analysis were compared with the ones obtained from the covariance step in NONMEM from the original data set. The visual predictive check was generated using 1,000 simulations from the final model, for all dose levels in our study, to assess the predictive performance and to verify if the performance is consistent among the dose levels. A graphical comparison was made between observed data and the model predicted median and 95% prediction interval over time.

Acknowledgments. This work was supported by CA112951, the Pharmacology Core of the University of Chicago Comprehensive Cancer Center (P30 CA14599) and the Indiana Clinical and Translational Sciences Institute (through a gift of Eli Lilly and Company).

Author Contributions. M.J.R., K.W., L.K.H., J.R., and R.R.B. wrote the manuscript; M.J.R. and E.E.W.C. designed the research; M.J.R., K.W., E.E.W.C., W.Z., and R.R.B. performed the research; and LKH and JR analyzed the data.

Conflict of interest. The authors declared no conflict of interest.

Study Highlights

WHAT IS THE CURRENT KNOWLEDGE ON THE TOPIC?
Previous pharmacokinetic studies of sirolimus in transplant patients reported linear pharmacokinetics.

WHAT QUESTION DID THIS STUDY ADDRESS?
In this study, we explored and described the nonlinearity of sirolimus using concentration data from patients with advanced solid tumors treated with a wide dose range (1–60 mg/week). We developed a PopPK model with saturable absorption characteristics.

WHAT THIS STUDY ADDS TO OUR KNOWLEDGE
This is the first PopPK report indicating the nonlinearity of sirolimus and the first PopPK report in patients with cancer.

HOW THIS MIGHT CHANGE CLINICAL PHARMACOLOGY AND THERAPEUTICS
Our model can be used to predict the effect of dose and/or schedule change on the whole blood concentrations of sirolimus. This will facilitate future studies of this agent inaddition to providing information that may guide dosing for patients individually.

1. Saunders, R.N., Metcalfe, M.S. & Nicholson, M.L. Rapamycin in transplantation: a review of the evidence. *Kidney Int.* **59**, 3–16 (2001).
2. Houchens, D.P., Ovejera, A.A., Riblet, S.M. & Slagel, D.E. Human brain tumor xenografts in nude mice as a chemotherapy model. *Eur. J. Cancer Clin. Oncol.* **19**, 799–805 (1983).
3. Eng, C.P., Sehgal, S.N. & Vézina, C. Activity of rapamycin (AY-22,989) against transplanted tumors. *J. Antibiot.* **37**, 1231–1237 (1984).
4. Houghton, P.J. & Huang, S. mTOR as a target for cancer therapy. *Curr. Top. Microbiol. Immunol.* **279**, 339–359 (2004).
5. Stallone, G. et al. Sirolimus for Kaposi's sarcoma in renal-transplant recipients. *N. Engl. J. Med.* **352**, 1317–1323 (2005).
6. Chan, S. Targeting the mammalian target of rapamycin (mTOR): a new approach to treating cancer. *Br. J. Cancer* **91**, 1420–1424 (2004).
7. MacDonald, A., Scarola, J., Burke, J.T. & Zimmerman, J.J. Clinical pharmacokinetics and therapeutic drug monitoring of sirolimus. *Clin. Ther.* **22 (suppl. B)**, B101–B121 (2000).
8. Djebli, N. et al. Sirolimus population pharmacokinetic/pharmacogenetic analysis and bayesian modelling in kidney transplant recipients. *Clin. Pharmacokinet.* **45**, 1135–1148 (2006).
9. Zahir, H., Keogh, A. & Akhlaghi, F. Apparent clearance of sirolimus in heart transplant recipients: impact of primary diagnosis and serum lipids. *Ther. Drug Monit.* **28**, 818–826 (2006).
10. Ferron, G.M., Mishina, E.V., Zimmerman, J.J. & Jusko, W.J. Population pharmacokinetics of sirolimus in kidney transplant patients. *Clin. Pharmacol. Ther.* **61**, 416–428 (1997).
11. Sato, E. et al. Temporal decline in sirolimus elimination immediately after pancreatic islet transplantation. *Drug Metab. Pharmacokinet.* **21**, 492–500 (2006).
12. Dansirikul, C., Morris, R.G., Tett, S.E. & Duffull, S.B. A Bayesian approach for population pharmacokinetic modelling of sirolimus. *Br. J. Clin. Pharmacol.* **62**, 420–434 (2006).
13. Jiao, Z., Shi, X.J., Li, Z.D. & Zhong, M.K. Population pharmacokinetics of sirolimus in de novo Chinese adult renal transplant patients. *Br. J. Clin. Pharmacol.* **68**, 47–60 (2009).
14. Cohen, E.E. et al. Phase I study of rapamycin (R) in combination with CYP3A4 modifier, ketoconazole (K), in patients with advanced malignancies. *J. Clin. Oncol.* **24** (**suppl. 18**), S3061 (2006).
15. Ratain, M.J. et al. A phase 1b study of oral rapamycin (sirolimus) in patients with advanced malignancies. *J. Clin. Oncol.* **25** (**suppl. 18)**, S3510 (2007).
16. Jonsson, E.N., Wade, J.R. & Karlsson, M.O. Nonlinearity detection: advantages of nonlinear mixed-effects modeling. *AAPS PharmSci* **2**, E32 (2000).
17. Beal, S.L., Sheiner, L.B.& Boeckmann, A.J. (eds.) NONMEM Users Guides. (1989–2006) (Icon Development Solutions, Ellicott City, MD, 2008).
18. Beal, S.L. Ways to fit a PK model with some data below the quantification limit. *J. Pharmacokinet. Pharmacodyn.* **28**, 481–504 (2001).
19. Yano, Y., Beal, S.L. & Sheiner, L.B. Evaluating pharmacokinetic/pharmacodynamic models using the posterior predictive check. *J. Pharmacokinet. Pharmacodyn.* **28**, 171–192 (2001).
20. Karlsson, M.O. & Holford, N. A tutorial on visual predictive checks. Annual Meeting of the Population Approach Group in Europe (PAGE), Marseille, France, 18–20 June 2008.
21. Trepanier, D.J., Gallant, H., Legatt, D.F. & Yatscoff, R.W. Sirolimus: distribution, pharmacokinetics and therapeutic range investigation: an update. *Clin. Biochem.* **31**, 345–351 (1998).
22. Mahalati, K. & Kahan, B.D. Clinical pharmacokinetics of sirolimus. *Clin. Pharmacokinet.* **40**, 573–585 (2001).
23. Zahir, H., McLachlan, A.J., Nelson, A., McCaughan, G., Gleeson, M. & Akhlaghi, F. Population pharmacokinetic estimation of tacrolimus apparent clearance in adult liver transplant recipients. *Ther. Drug Monit.* **27**, 422–430 (2005).
24. Wu, K.H. et al. Population pharmacokinetics of cyclosporine in clinical renal transplant patients. *Drug Metab. Dispos.* **33**, 1268–1275 (2005).
25. Lamoureux, F., Picard, N., Boussera, B., Sauvage, F.L. & Marquet, P. Sirolimus and everolimus intestinal absorption and interaction with calcineurin inhibitors: a differential effect between cyclosporine and tacrolimus. *Fundam. Clin. Pharmacol.* **26**, 463–472 (2012).
26. Cummins, C.L., Jacobsen, W., Christians, U. & Benet, L.Z. CYP3A4-transfected Caco-2 cells as a tool for understanding biochemical absorption barriers: studies with sirolimus and midazolam. *J. Pharmacol. Exp. Ther.* **308**, 143–155 (2004).
27. Vrijens, B., Tousset, E., Rode, R., Bertz, R., Mayer, S. & Urquhart, J. Successful projection of the time course of drug concentration in plasma during a 1-year period from electronically compiled dosing-time data used as input to individually parameterized pharmacokinetic models. *J. Clin. Pharmacol.* **45**, 461–467 (2005).
28. Ahn, J.E., Karlsson, M.O., Dunne, A. & Ludden, T.M. Likelihood based approaches to handling data below the quantification limit using NONMEM VI. *J. Pharmacokinet. Pharmacodyn.* **35**, 401–421 (2008).
29. Yatscoff, R., LeGatt, D., Keenan, R. & Chackowsky, P. Blood distribution of rapamycin. *Transplantation* **56**, 1202–1206 (1993).
30. Yatscoff, R.W., Wang, P., Chan, K., Hicks, D. & Zimmerman, J. Rapamycin: distribution, pharmacokinetics, and therapeutic range investigations. *Ther. Drug Monit.* **17**, 666–671 (1995).

Supplementary Information accompanies this paper on the *Pharmacometrics & Systems Pharmacology* website (http://www.nature.com/psp)